Recovering wide angular sector multibeam backscatter to facilitate seafloor classification

Aluizio Maciel de Oliveira Junior[1, 2] and John E. Hughes Clarke[1]

1. Ocean Mapping Group (OMG), Dept. of Geodesy and Geomatics Engineering, University of New Brunswick
2. Directorate of Hydrography and Navigation (DHN), Brazilian Navy

Abstract

Due to a focus on bathymetric data quality over backscatter imaging quality, multibeam angular sectors greater than +/- 60° are rarely used in hydrographic surveys. Wider sector data are prone to refraction and motion errors, and the along-track sounding density is reduced, thereby potentially compromising target detection. For the purposes of seafloor classification using power spectral analysis (Pace and Gao, 1988) however, the wider sectors provide significant advantages. The Brazilian Navy has routinely been operating EM1000 sonars using a roll-stabilized +/-75° sector with 200% coverage, allowing the potential for implementing such classification. The EM1000 system furthermore, logs the outermost beam intensity time series well beyond the half beam width. New software has been developed to take advantage of this extra coverage beyond the last beam resulting in up to 28% increased area coverage.

If properly compensated for beam pattern residuals, this expanded coverage represents an improved capability to attempt power spectral classification. This approach is demonstrated herein, illustrating the method of outer trace extraction, beam pattern correction and practical application of power spectral analysis.

These algorithms have now also been extended to include the new EM710. This new sonar provides two advantages over the older EM1000 that are important for application of the power spectral analysis method; the effective transmit beam width is much tighter (2.4° v. 0.5°) resulting in an along-track dimension closer to the range resolution, and the EM710 also has the potential to have multiple along-track swaths within a single ping cycle, which gets around the requirement of narrowing the angular sector to achieve tight along-track spacing.

1. Introduction

Multibeam backscatter has been used extensively as a source for seafloor classification (see range of references at end). The backscattered energy that returns to the ship depends both on the seafloor physical properties themselves and also on the sonar configuration, water column propagation and measurement geometry. These last geometric and radiometric modulations on the backscatter intensity must be reduced, such that the backscatter strength might become a useful signal for the task of seafloor physical properties characterization.

There are a variety of approaches to multibeam backscatter classification including textural methods (e.g. grey-level co-occurrence matrixes, Pace and Dyer, 1979, Reed and Hussong, 1989, Haralick, 1979 and Imen et al., 2005), angular response characterization (e.g. deMoustier and Alexandrou, 1991, Matsumoto et al, 1993 and Hughes Clarke, 1994) and power spectral methods (Pace and Gao, 1988, Tamsett, 1993 and Lurton et al., 1994). Textural methods tend to ignore the imaging geometry, working mainly on the mosaiced intensity data, thereby implicitly assuming that neither the grazing angle nor the imaging azimuth is important. Angular response characterization examines the variation with grazing angle, averaged over half a swath width, thereby implicitly only classifying regions larger than a typical swath width. In contrast to both of the other methods, power spectral classification works specifically along the ping azimuth, deliberately avoiding high grazing angle data and can be used to attempt to classify multiple sediment types within a single swath. Thus to use power spectral methods, one needs to collect data at lower grazing angles, as was the case for the low aspect ratio sidescan systems.

For the case of typical hydrographic-purpose multibeam acquisition, however, the backscatter data collection has been usually restricted to high grazing angles, because bathymetric target detection requirements demand the better along-track coverage gained with the swath reduction. Furthermore low grazing angles are more susceptible to the refraction and motion errors. As a result, most multibeam backscatter has been explored within smaller incidence angle sectors while sidescan sonar imagery explores the higher incidence angles. Some attempts to use power spectral classification at high grazing angles (e.g. Kavli et al., 1993 (built into the Simrad Poseidon software), or Quester Tangent, 2006) have been made, but are strongly

limited by the rapid changes in intensity due to seafloor slope variations approaching normal incidence. Ideally data should be collected out to lower grazing angles generally beyond the critical angle (~61º for 1700m/s (sediment P-wave sound speed), ~70º for 1600m/s) to take best advantage of power spectral classification.

The Brazilian Navy decided to use their EM1000 sonar installed in the Hydrographic Ship Taurus in the equiangle beam spacing (EABS) 150º mode (~7.5x the water depth) with 200% coverage for the last 7 years, nearly twice as wide as most other hydrographic operators. The purpose was to keep an enhanced beam density in the inner regions while simultaneously using the sparse outer beams distribution as a means of detecting refraction problems during survey. This provides an indicator for when it might be necessary to obtain new sound velocity casts. A serendipitous byproduct of this policy, however, was the collection of additional extra valuable backscatter information that is suitable for spectral classification methods. To be used for this purpose, however, the data need to be properly reduced for geometric and radiometric artefacts.

Previous works (Hellequin et al., 1997 and 2003) described the processes involved in EM1000 backscatter artefact cleaning for the case of equidistant beam spacing (EDBS). In this beam spacing mode, particular attention needed to be paid to the fact that the inner beams were spaced much wider than their -3dB beam widths. With the EABS data collected herein, the main focus of the backscatter artefact cleaning is to cope with the outer beams artefacts. These resulted from the system logging additional backscatter data beyond the half beam width of the outermost beam. A pleasant byproduct of this extra logging is that the effective backscatter swath width markedly increased and, as 200% coverage was used, this allowed complete overlap of the nadir beams of the adjacent lines with the low grazing angle backscatter data.

Taking advantage of the wider swaths and the available lower grazing angle data, two new developments are presented here:

First, an alternative approach for mosaicing data was implemented in which a range weighting function was used to favour outer beams with respect to the inner beams (the reverse of the usual mosaicing process). This procedure enhanced the quality of final mosaic and suppressed the along-track artefacts that are normally overprinted on the mosaics.

Secondly, the artefact-reduced low-grazing angle backscatter strength was evaluated through a power spectral classification toolkit that was originally created to work with conventional sidescan sonar data (Hughes Clarke, 2004). The software was adapted to accommodate multibeam data, allowing the detection of image pixels corresponding to the swath external limits and accounting for the depth oscillations effects. The inner angular limits can be selected to avoid the low incident angles. The schema used was capable of producing regularly-spaced classification boxes recovering the entire seafloor.

In addition, the same algorithms created for the EM1000 process have now been implemented for the much newer EM710 sonar (at this point, with the configuration using only one profile per ping cycle). In the near future, it is planned that these newer sonars will allow double across-track swaths per ping cycle, thereby bypassing the requirement of narrow swaths to achieve good along-track density.

2. Datasets used in the Experiment

Two datasets were used during software implementations:

1) First dataset: collect by the Brazilian Navy with the Hydrographic Ship Taurus from 31/aug/2004 to 07/sep/2004. A Simrad EM1000 multibeam operating in the EABS 150^{o} mode was used to survey Barra do Riacho, ES, Brazil.

2) Second dataset: collect by the Canadian Hydrographic Service with the CCGS Matthew in 15/may/2006. Used a Simrad EM710 multibeam in the EDBS 65^{o} mode. In Esquimalt area, offshore of Halifax Harbour.

3. Outer Beams Backscatter Traces

The EM1000 beams are formed by the product of the transmitted 3.3^{o} along-track beamwidth beams and the 60 received beams which have 3.3^{o} along and across-track beamwidth. The fore-aft product between transmitted and received beams generates an effective 2.4^{o}

beamwidth along-track. Away from vertical incidence, the across-track resolution is controlled by the pulse length which is 0.2 ms, equivalent to 15cm.

During the acquisition of the raw intensity time series for each beam, data well before and beyond the projection of the half-beamwidth (-3dB limit) are recorded. When the data are subsequently stored, overlapping inner beams have redundant data and thus normally only the data within the -3dB limits are generally retained. If, however, an inner beam is dropped, the beam traces on either side are lengthened just enough into the intervening time gap to ensure a continuous coverage. For the outermost beams, however, for which there is never an adjacent beam outboard, the full beam trace outboard is retained, resulting in potentially a much wider available backscatter swath.

In Figure 1, the 60 beams coverage for the EM1000 operating in the EABS 150^{o} mode is highlighted through different colours. The outer beams importance is visually evident. Note the shifted position of transmission direction between pings that is caused because the transducer uses alternately offset beam steering angles for subsequent pings (offset by ½ a beam width – sometimes referred to as "beam hopping").

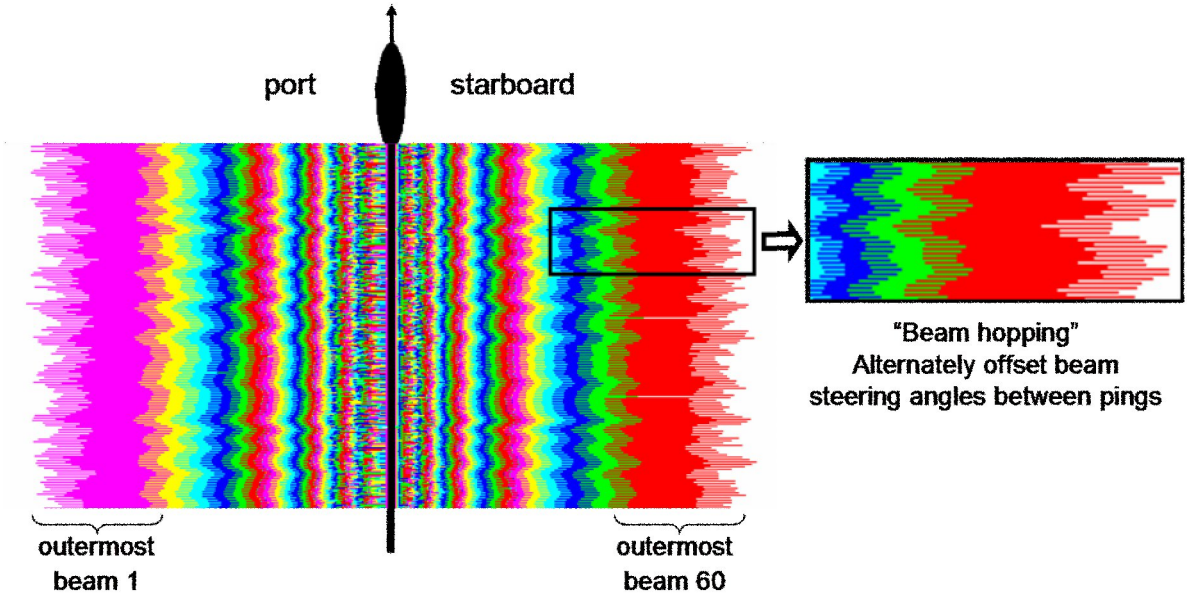

Fig.1: The 60 beams of the EM1000 operating in the equiangle 150^{o} mode and the evident importance of the outer beams coverage area. Note the disproportionately large extent of the outermost beams trace. The beam bottom strike is usually in the centre of the time series for most beams, but for the outermost beams lies well toward the inboard edge.

3.1. Analysis and reduction of beam-pattern artifacts

Considering the imaging geometry presented in Figure 2, one can observe that the total number of samples within each beam is a function of the beam launch angle (θ) and depth. In the vertical incidence situation, beam instantaneous footprint is limited by the across-track beamwidth. Otherwise, as the incidence angle increases, beam pulse length is the main factor which restricts the instantaneous footprint. Therefore, higher incidence angles, as well as greater depths, are capable of increasing the number of samples stored inside each beam. The consequence of storing more samples is the tighter launch angle interval between samples. Equation 1 was used to compute the samples launch angles considering the geometry presented.

$$\theta_{sample} = \left(\frac{depth * \cos(\theta_{centre})}{depth + (sample\_length * (sample\_number - centre\_number) * \cos(\theta_{centre})} \right) \qquad \text{(Eq.1)}$$

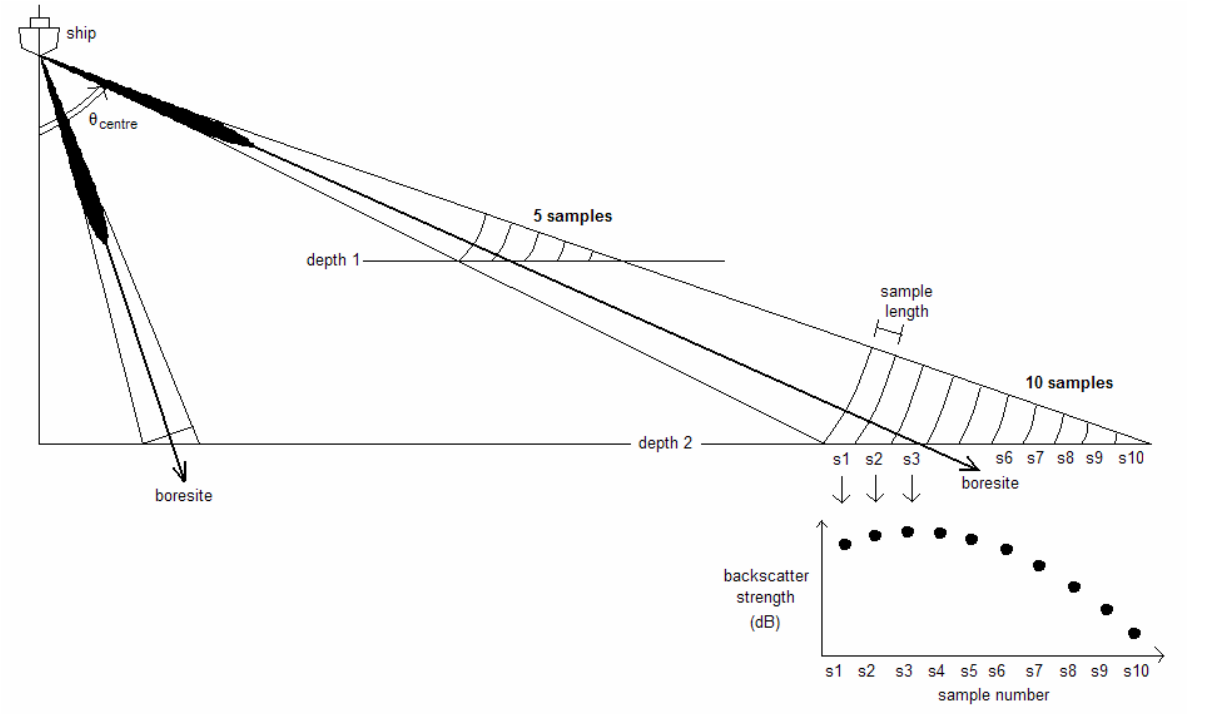

Fig.2: The imaging geometry. Inner beams are limited by beam width and outer beams store many instantaneous footprints (samples). The number of stored samples is a function of the beam launch angle and depth.

Backscatter intensities plotted as a function of launch angle as presented in Figure 3. Intensities are just taken from Simrad's sonar image datagram and are mapped according to their launch angle. The straighter (and red) line shows the results when using the OMG's *beampatt* algorithm which averages the backscatter for each 1.0 degree interval. The other line (in black), with many oscillations, represents the method implemented here, using the *tracepatt* algorithm, which works inside each beam and computes the averages for each 0.1 degree interval. Notice that each beam stores a range of 2-3dB, but outermost beams are able to extend their range more than 10dB. Beam pattern reduction was implemented for all the beams because it would represent an improvement in the final power spectral analysis. However, main emphasis has been delivered to the outermost beams as they implemented the useful backscatter range up to 28%. Furthermore, they are the most important tool used in the mosaicing and classification steps.

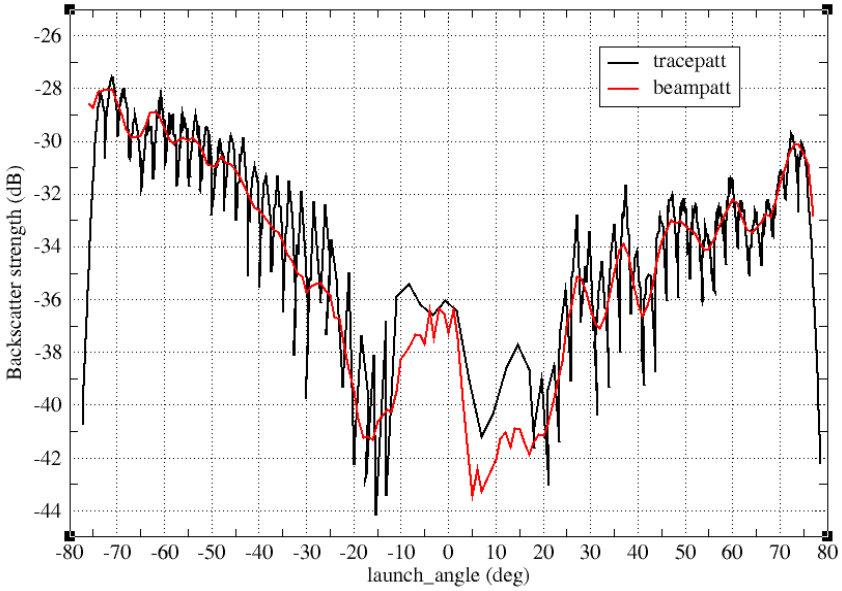

Fig.3: Original backscatter strength amplitude time series taken from Simrad's sonar image amplitude telegram. Tracepatt works inside each beam and calculates the average backscatter strength within a 0.1 degrees interval. Beampatt averages amplitudes each 1.0 degrees interval.

For beam pattern reduction, the least squares fitting technique is applied for the determination of the equation parameters that are used to normalize the traces amplitudes. An example is showed in Figure 4 that was produced during the processing of the port outermost beam trace amplitudes.

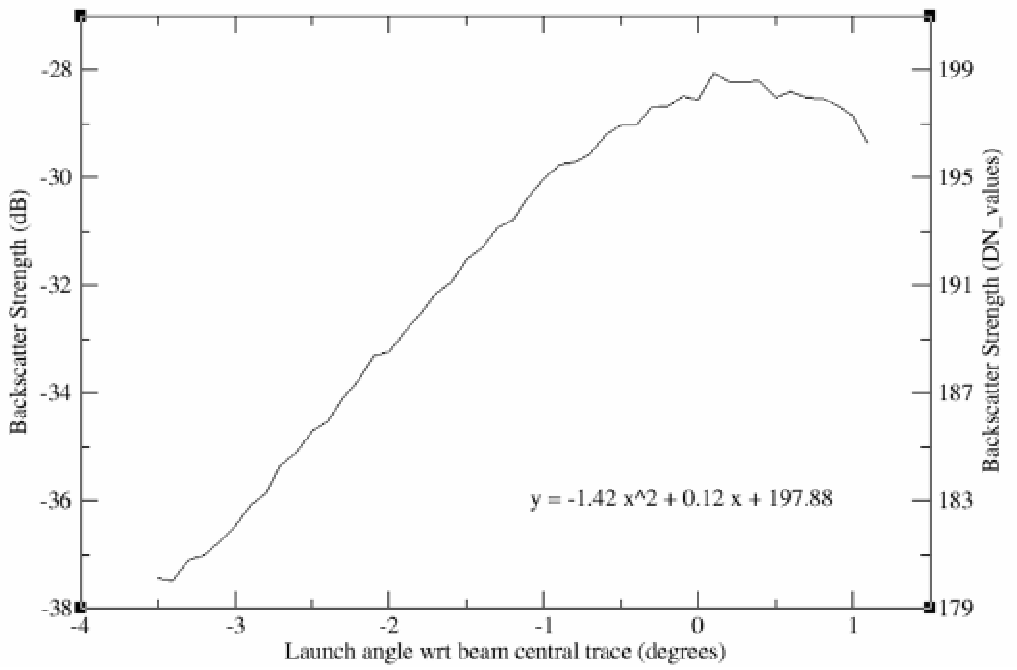

Fig. 4: Port outermost beam pattern calculated from the average backscatter strength taken each 0.1 degrees launch angle intervals and corresponding quadratic equation calculated with least squares fitting method.

Figure 5 shows the backscatter maps in different processing steps. Images were taken from a region crossing two pipelines. First, the raw backscatter (Figure 5a) has many artifacts printed in the along-track direction of the survey line. OMG software was applied to reduce beam-averaged geometric and radiometric artefacts due to the sediment angular response and the beam-to-beam pattern effects (transmit and receive directivity). This therefore only deals with the average backscatter strength for each beam (it assumes no significant variation within a single beam). As there is, in fact, a significant beam pattern residual in the outermost beams, there remains a visibly (artifact 4) uncompensated roll-off in the last beam trace (Figure 5b). Without removing this, the extra 28% of the data cannot be used effectively for either mosaicing or power spectral analysis. To correct for this, an additional step was implemented for processing the outermost beams to increase the usefulness and final quality of the image (Figure 5c). In addition, small oscillations within each of the other beams were also compensated.

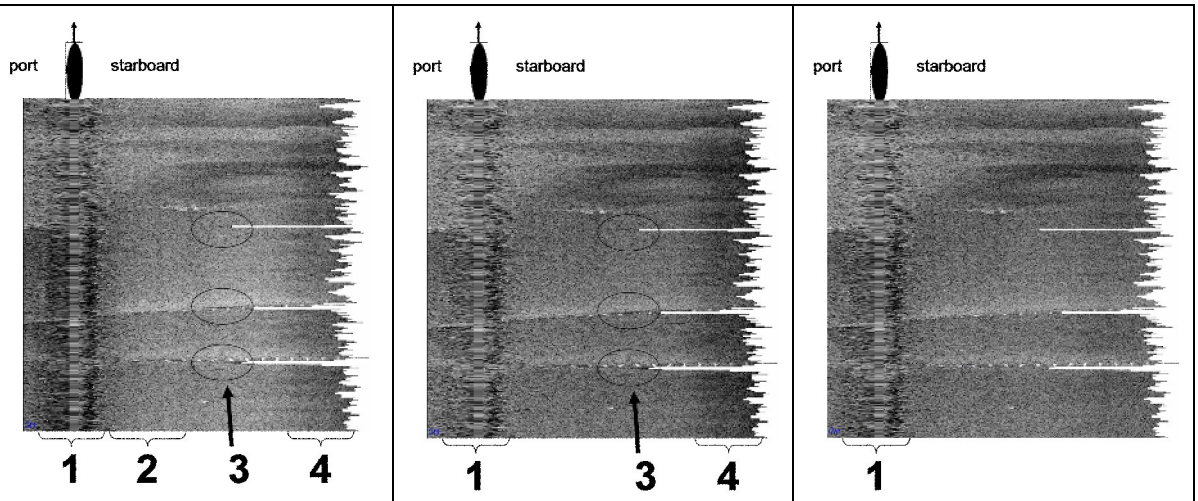

(a) raw backscatter strength	(b) preliminary processing with OMG *beampatt* software (reduce angular response effect and beam-to-beam artifacts)	(c) implemented process using *tracepatt* software (reduce inside-beam pattern artifacts)

Fig. 5: Backscatter maps taken from different processing steps.

(Fig. 5a): Raw backscatter presents plenty of artifacts: noisy inner region (artifact 1), strong beam-to-beam oscillations (artifact 2), losing beam tracking close to the pipelines and topographic slopes (artifact 3) and rolling down intensities in the outermost beams (artifact 4).

(Fig. 5b): Preliminary processing using *beampatt* software was able to reduce the strong contrast across the swath (between the 4 artifact regions described), normalizing the backscatter strength values accounting for the angular response and beam-to-beam artifacts. Notice that artifact 2 is also reduced.

(Fig. 5c): Implemented processing using *tracepatt* software worked mostly on the artifacts 3 and 4, related to the strong backscatter oscillation taking place within each beam. In the case of the outermost beams, strong variations are normally present. In the case of other beams, oscillations stronger than 2-3dB (more visible in the image) occur when the sonar loses the seabottom tracking and a gap is formed between the beams.

3.2. Filling the outermost beams "hopping" gaps

As a result of the beam hopping, the outermost coverage is strictly not completed. Therefore, there is the necessity of filling the hopping gaps, which takes place at the end of the processing steps to allow the usage of the maximum portion of the swath.

Figure 6a presents the raw intensities in the starboard outermost beam location with the hopping gaps already present. Figure 6b shows the results after reducing data artifacts. The last image, Figure 6c, demonstrates the effect produced after filling the gaps between the pings.

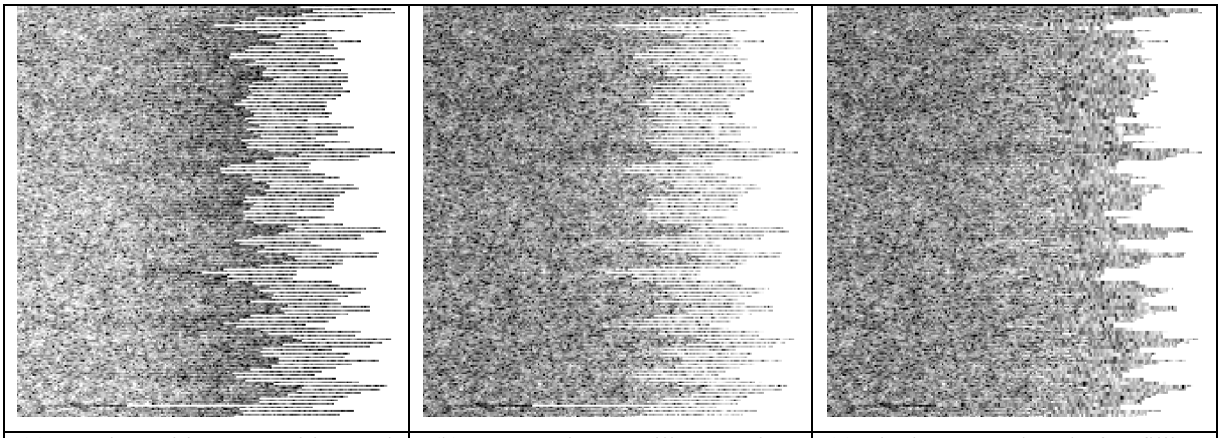

(a) Raw intensities map, with actual coverage of outermost beams. Presents the gaps and backscatter roll-off (dark).	(b) Processed map, still presenting the original coverage (with the gaps), but roll-off is reduced.	(c) Final map produced after filling the gaps.

Fig. 6: Process of filling the gaps in the outer beams.

3.3.Testing the usefulness of implemented process for power spectral analysis

After the end of processing steps and filling hopping gaps, the OMG *sslook* tool was used to enable a closer look in the validity of using the outer traces that were normalized and filled for classification. By comparing the power spectra of regions of the seabed both in the middle and outer part of the swath (two boxes in Figure 7), we are able to confirm that the spectra normally indicated the effectiveness of the applied process for artifacts reduction.

The *sslook* tool (Hughes Clarke, 2004) automatically extracts a ground-range corrected intensity profile over a user-selected length and number of immediately-adjacent pings. For each profile, an FFT is performed to look at the power spectra. All spectra for the user-specified number of pings are averaged and the resulting average power spectra are then available for analysis (Pace and Gao, 1988).

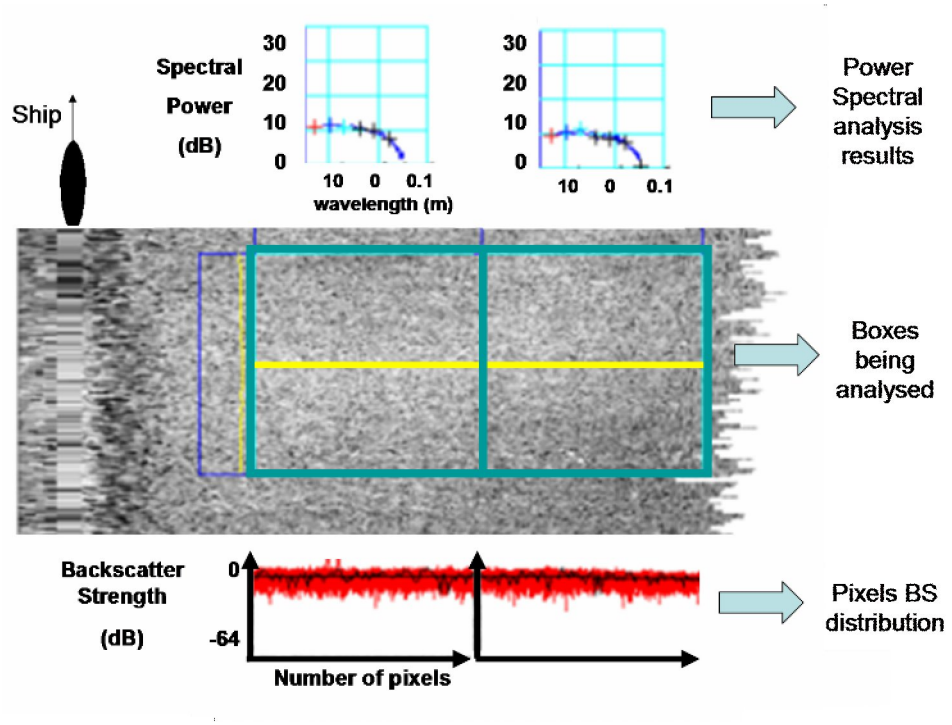

Fig. 7: Power Spectral comparison between boundary and central boxes.

4. Mosaicing the Outer Beams with Higher Weights

Most automatic sidescan mosaicing software has the ability to deal with inter-swath overlap. Because the outermost part of the swath is often noisy, the default is to preferentially overlay inner swath data over outer swath data. This tends to retain the near-nadir variations in backscatter strength which have a very strong and sensitive dependence on seabed slope. For the purpose of regional sediment mapping, it is preferable to have sidescan/backscatter data that is at lower grazing angles. As we are collecting 200% coverage and have now removed the outermost beam pattern artefacts, we have the opportunity to replace the high grazing angle data. Mosaicing weights were established giving more importance for the outer beams. A ramp function was created with outer beams having maximum values and the inner beams with lower values weights.

The image presented in Figure 8a was processed using the default method and Figure 8b shows the results of changing the weights.

The leftmost image is dominated by the "nadir stripe". Although the average variation in beam pattern, across the swath has been compensated for, there is a markedly different texture at nadir that still draws the eye. Part of the problem is that the shape of the near-nadir angular response curve is highly sediment dependent and thus averaging that over a survey line (crossing multiple sediment types) fails to account for local changes in the angular response.

In the rightmost image, where the outermost swath data of the adjacent line covers the nadir region, it has been replaced. A markedly-reduced contrast in the along-track striping in the image is evident. The line spacing, however, is not always achieving 200% coverage and occasional near nadir data is retained. Without correcting for the roll-off in the outermost beam pattern, this would not be possible.

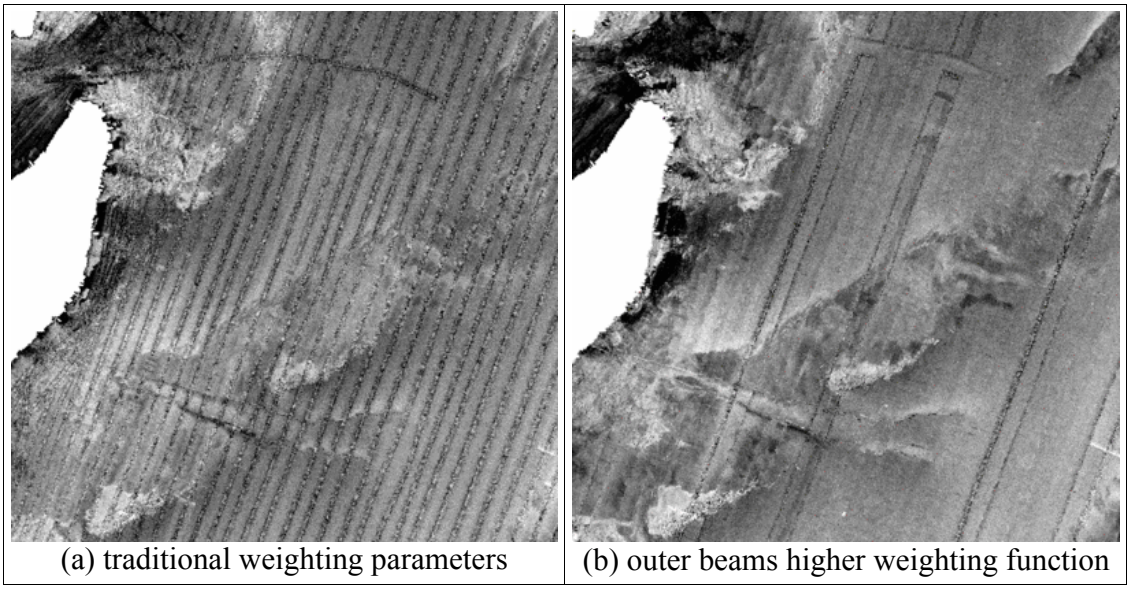

(a) traditional weighting parameters (b) outer beams higher weighting function

Fig. 8: Backscatter mosaics from the harbour area prepared using two different weighting parameters.

5. Implementing Power Spectral Boxes for Seafloor Classification

The power spectral method for seafloor classification was first demonstrated by Pace and Gao (1988). Their results with sidescan sonar backscatter suggested up to 97% success in classification. They used statistical features created with the ratios between different spectral ranges. Significantly they dealt with low-aspect ratio sidescan data and specifically avoided the near nadir backscatter data (which is only a small percentage of the swath).

More recently, the OMG developed *classSS* software (Hughes Clarke, 2004) to deal with a keel mounted sidescan sonar situation. This reproduces the Pace and Gao approach with the single important addition of looking at the average backscatter strength. The Pace and Gao method had normalized all spectra to the peak level as the early sidescan sonar data had automatic gain control and thus the mean value had no classification significance. This program was adapted in this study to accommodate the multibeam sonar characteristics, which works in a different angular sector.

Software modifications implemented by the first author had to cope with the irregular swath width and higher aspect ratio of multibeam sonar backscatter. These modifications included a function to detect outer beams range to become the start point of the classification boxes creation, therefore accounting for depth oscillations during the survey. The boxes have their size defined by the user (number of pixels across-track and number of pings in the along-track direction). The inner incidence angle limit can also be chosen to avoid the noisy central region. The number of classification boxes across the swath is therefore not constant. Rather it is dynamically varying to address just the most appropriate data.

During backscatter processing, pixels were generated with 0.15m radial dimension to match the sonar pulse length that determines the across-track resolution. Power spectral boxes were created with 128 pixels, so each box has an across-track dimension of 19.2m, corresponding to the maximum spectral wavelength that can be determined in this case. The along-track size is determined by the number of pings, which was established as 16 pings. Vessel average speed was ~4m/s and ping rate of 3.3 pings per second, so along-track box dimensions are ~19.4m. Therefore, classification boxes used were almost squared with sides approximately ~19m. In Figure 9 the boxes are represented in the sidescan strip before geo-referencing, having the compression effect in the along-track direction. The red full-line registered in the top of the image is created to signal an invalid stack of pings eliminated from the classification procedures.

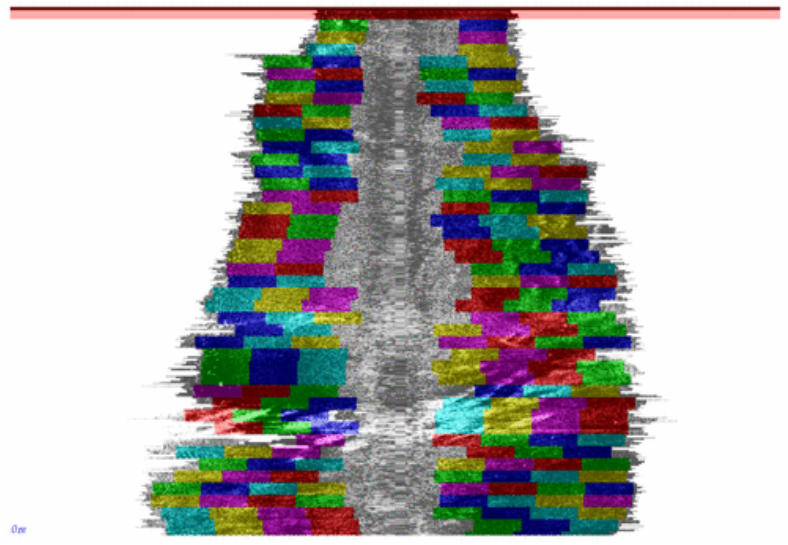

Fig. 9: Classification Boxes with outer limits of 75° and inner limits of 30°. Boxes across-track sizes of 128 pixels (each pixel with 0.15m) and along-track sizes of 16 pings (vessel at ~4m/s and ping rate ~3.3Hz). It adjusts to the depth variations. Red full-line is a flag-out signal because of invalid ping occurrences, therefore stack is discharged.

The software was used to process all the survey lines. For each ~19x19m patch, a series of parameters are extracted including the average backscatter strength, standard deviation and 7 representative spectral powers. The final processed backscatter mosaic for the entire surveyed area is represented in Figure 10a, where four distinct regions are indicated: (1) shoreline, (2) intermediate, (3) offshore and (4) pipelines location.

The first products delivered by the classSS software are the statistical maps that give the average and standard deviation maps, computed for backscatter strength values inside each classification box. The average map could enhance the contrast between different regions when compared to the normal mosaic. This is the prime output of most regional backscatter mosaics. It is only a valid classifier if radiometric and geometric corrections have been applied. Already, clear sediment boundaries are visible. However, based on the ground truth data, we know that multiple sediment types can produce the same mean backscatter strength. We therefore wish to better separate these sediment types through the use of more degrees of freedom. The standard deviation map (Figure 10b) was able to enhance regions with strong textural signature. The pipelines location (region 4) was highlighted when compared to the other maps (including to the sun illumination bathymetric map).

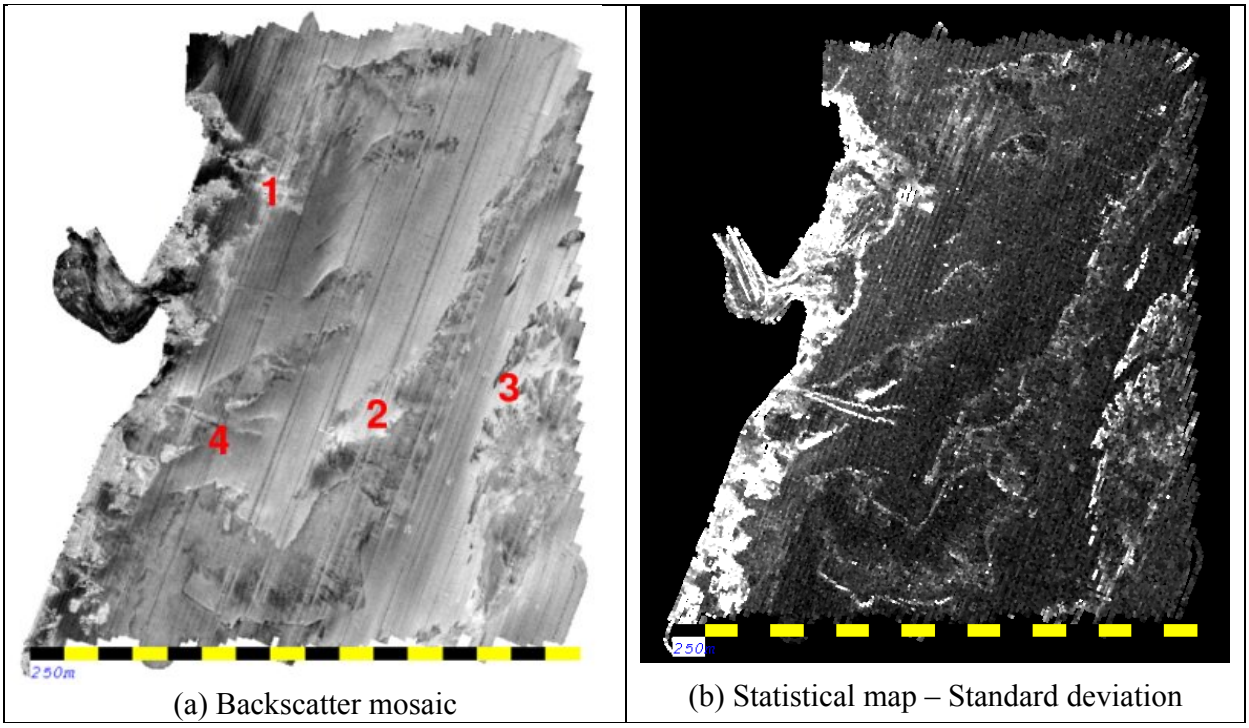

(a) Backscatter mosaic (b) Statistical map – Standard deviation

Fig. 10: Maps produced during processing steps.

The other degrees of freedom available from the classification method are the power spectral maps. Seven maps representing the spectral wavelengths of 19.2m, 9.6m, 4.8m, 2.4m, 1.2m, 0.6m and 0.3m are generated. The wavelength can represent either topographic characteristics (changes in seabed slope at the limit of, or below, the resolvable bathymetric resolution) or seabed patchiness (changes in seabed type). The spatial variability in particular physical properties (impedance, roughness and volume inhomogeneity) produce power oscillation in different frequencies.

Results demonstrated that power spectral maps can add contribution to seafloor type segmentation. When comparing the areas under the number 1, 2 and 3 on Figure 10a, one sees they have similar average backscatter and therefore cannot be segmented using mean backscatter strength alone.

Analysing the power spectral maps (Figure 11) though, these regions can be properly segmented as having distinct characteristics. In Figure 11a (19.2m wavelength) all the regions still are similar. But, in the Figure 11b (9.6m wavelength) the intermediate region 2 is

represented as having lower energy in this frequency. Continuing to the next Figure 11c (4.8m wavelength), the offshore region 3 loses energy and it becomes indistinct to the intermediate region 2. While wavelengths are reduced more seafloor facies disappear. In the sixth spectral map presented in the Figure 9d (0.6m wavelength), no more distinction can be observed between the areas.

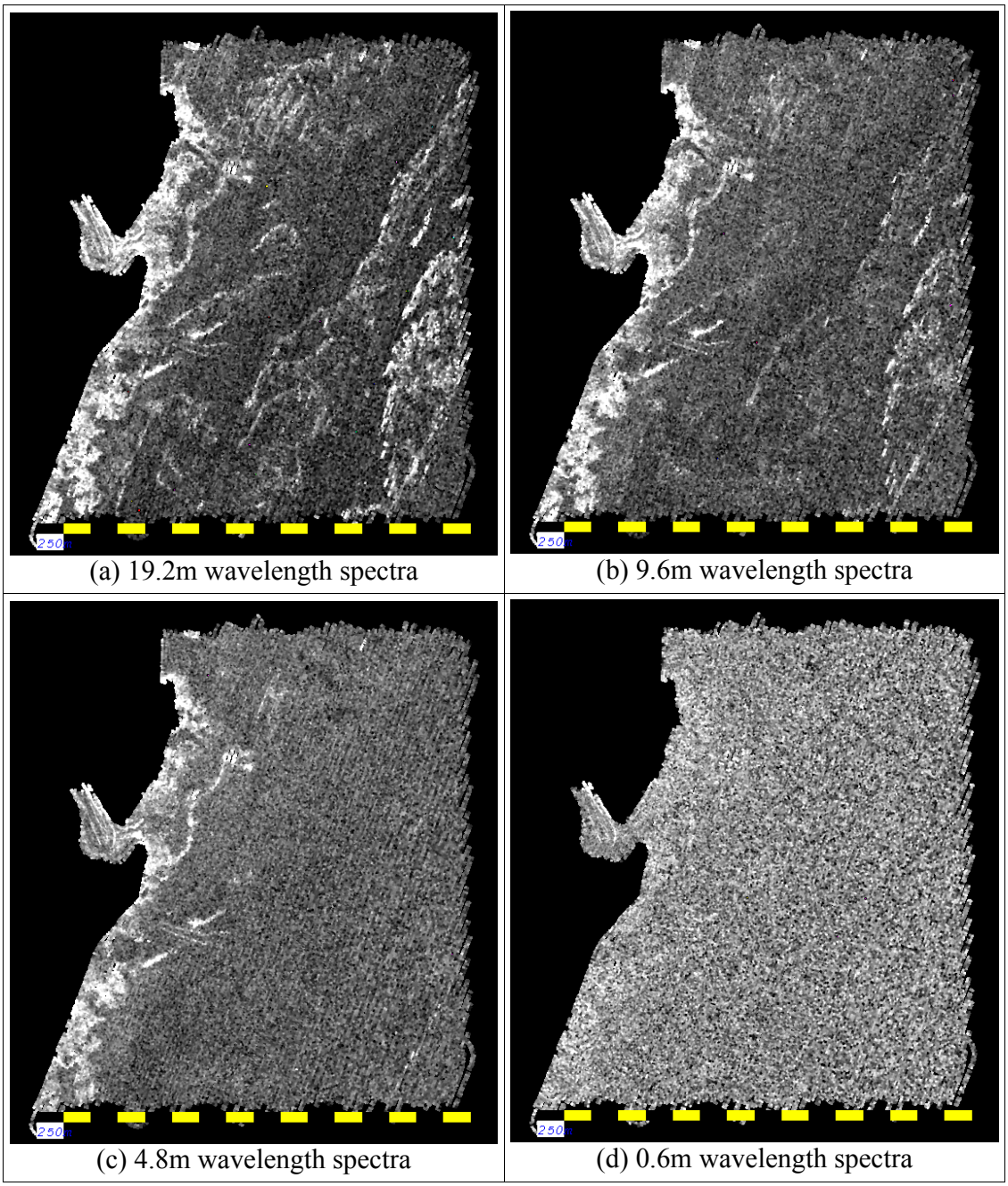

(a) 19.2m wavelength spectra (b) 9.6m wavelength spectra

(c) 4.8m wavelength spectra (d) 0.6m wavelength spectra

Fig. 11: Power spectral maps showing energy concentration within different wavelengths.

Similar results were found by Hughes Clarke (2004) when wavelengths smaller than 0.8m (~5x the pulse length) could no longer be used to segment different sediments. At this level, speckle phenomena compete with real patchiness in contributing to the backscatter variability. Therefore, as the pulse length is related to the minimum scale of patchiness that can be detected, we should suppose that sonars with 4 times larger pulse lengths than the EM1000's sonar 0.15m pulse length should still produce equivalent spectral maps. This is an important result as many of the multibeam sonars automatically change pulse length with signal to noise and we wish the classification scheme to be equivalent at all pulse length settings.

Although the within-beam pattern correction is mostly used in the outermost beams, under conditions where inner beams occasionally mistrack, the backscatter data includes anomalous low backscatter zones in the place of dropped beams. Although this does not grossly alter the look of the data, these low BS zones can alter the spectral signatures, providing false spectral energy and wavelengths close to the beam spacing. By applying the within-beam correction to all beams, these inter-beam gaps are removed and the spectral signatures are more faithful.

6. Future Perspectives on Backscatter Recording

Modern sonars like the EM710 are starting to operate with multiple across-track swaths within each ping cycle, which should represent the end of the necessity of reducing swath width to get the better along-track coverage. Figure 12a shows the effect of increasing the angular sector from 60^{o} to 75^{o}, when the larger two-way-travel time forces ping interval to increase. Therefore, along-track coverage density is reduced. In the other hand, wider angular sector (75^{o}) allows to increase the across-track coverage. Figure 12b presents the sonar capable of transmitting multiple along-track swaths per ping and their ability to maintain simultaneous across-track and along-track coverage.

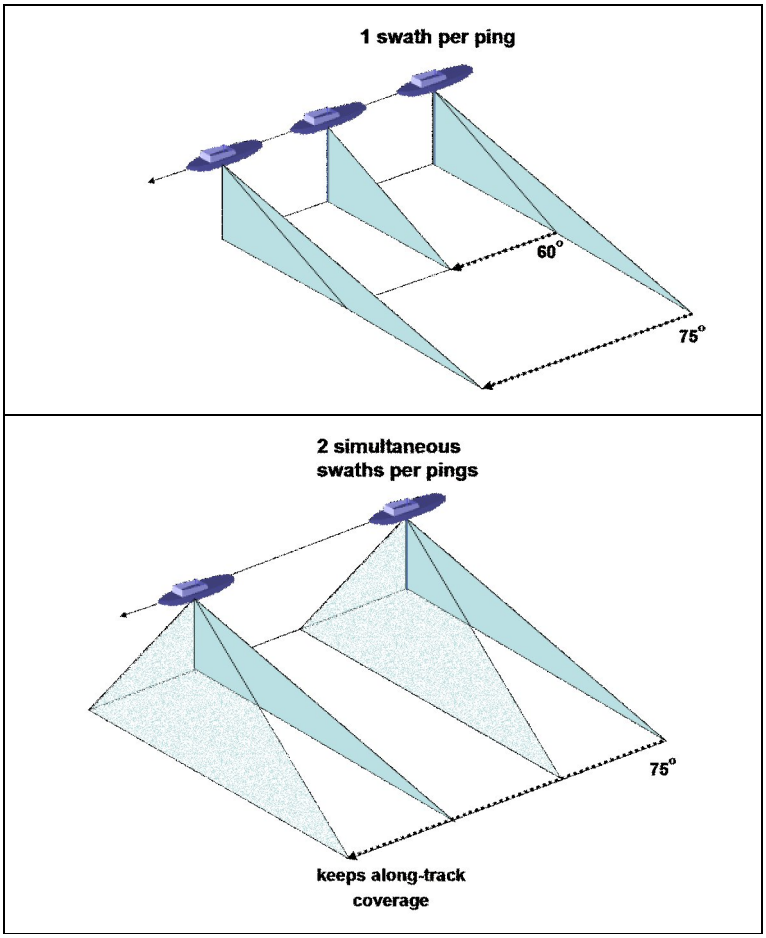

Fig. 12: (a) Sonar with single across-track swath per ping cycle: The wider (75°) angular sector causes the reduction in ping frequency, which generates along-track gaps in the survey coverage. In the other hand, the narrow (60°) angular sector enables the ideal along-track coverage, but compromises the across-track coverage. (b) Sonar with multiple across-track swaths per ping cycle: the simultaneous swaths per ping permits to get both the along-track and across-track coverage when operating with wider (75°) angular sectors.

Therefore, with multiple swaths sonars, the extended outer traces logged should represent additional valuable data to be processed for seafloor classification purposes. When the outer beams launch angle is increased, the percentage of coverage of the seafloor with relation to the total swath is also increased.

With these perspectives, sample EM710 data were collected (with only one swath per ping at this time) and processed to bring a first overview of the possibilities that should be taken with this system. Data was acquired on-board Canadian Coast Guard Ship Matthew operating in the proximities of Halifax Harbour.

The Figure 13 illustrates the beams pattern and the extended sector (~8%) reached when operating with only 65º maximum launch angle. The smaller extension of the coverage by using the outermost beam reflects both the more vertical incidence angle of the last beam (65º v. 75º) and the reduced receiver beam width (1.0º v. 3.3º)

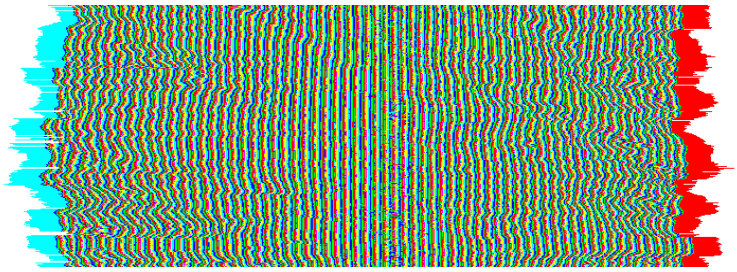

Fig. 13: The EM710 beams operating in the EDBS 65 mode with 1º x 0.5º beams. Outermost beams backscatter trace amplitudes correspond up to ~8% of the total swath.

The same processing steps applied for the EM1000 were followed for the EM710 and results also demonstrated its validity. The pattern found for the port outermost beam is represented in Figure 14, where recorded data ranges over the beam -3dB limits sector, giving an ensonified area with ~2.2º effective beamwidth, while other beams have only 1.0º across-track beamwidth.

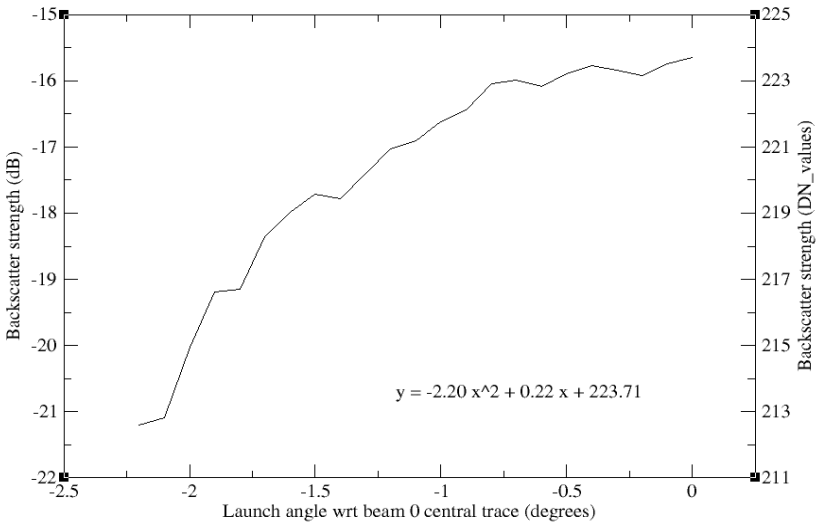

Fig. 14: Port outermost beam average backscatter strength calculated for each 0.1 degree launch angle interval and quadratic equation obtained with least squares fitting method to be used for amplitude normalization.

The implementation permits the usage of an extended region of the swath at, and beyond, the critical angle. The reason that it is useful to collect data beyond the critical angle is that volume scattering phenomena, that can overprint the backscatter inside the critical angle, is absent. Depending on the ratio between the compressional sound speed of each specific sediment type and the water sound speed, the critical angle would be defined. Beyond the critical angle, insignificant acoustical penetration takes place therefore volumetric inhomogeneities can be discharged, so roughness properties prevails. This allows a near equivalent classification to that achieved using low-aspect ratio sidescan sonars.

7. Conclusions

The aim of this research project was to demonstrate the efficacy of utilising the available low grazing angle backscatter data, not normally collected in multibeam operations. Outer beams intensity time series that are logged beyond the range of the beam centre limits were analysed and results demonstrated they present a regular patterns which can be satisfactorily reduced in order to allow its application for both improving mosaicing and seafloor classification purposes using power spectral analysis.

The methods represent an improvement of processing capabilities for the Brazilian Navy that has used EM1000 within equiangle 150^{o} mode and 200% survey lines coverage for about 7 years. Furthermore, it demonstrates the future potential for the newer sonars like the EM710 with multiple across-track swaths per ping cycle, because they get around the requirement of narrowing the angular sector to achieve high ping concentration in the along-track direction.

Acknowledgments

Data was provided by the Brazilian Navy (collected by the Hydrographic Ship Taurus) and by the Canadian Hydrographic Service (collected by the CCGS Mathew). The assistance of Mike Lamplugh of the CHS and Lt. Cmdr. Jim Bradford of the Canadian Navy are most

appreciated. This research was funded through the industrial sponsorship of the Chair in Ocean Mapping at UNB. Sponsors include the U.S. Geological Survey, Kongsberg Maritime, the Royal (U.K.) Navy, Fugro Pelagos, Rijkswaterstaat and the Route Survey Office of the Canadian Navy.

References

Augustin, J.M., et al, 1996, "Contribution of the Multibeam Acoustic Imagery to the Exploration of the Sea-Bottom", *Marine Geophysical Research,* v.18, p.459-486.

Augustin, J.M., and Lurton, X., 2005, "Image Amplitude Calibration and Processing for Seafloor Mapping Sonars", *IEEE Oceans'2005 Europe Conference Proceedings*, vol. 1, p. 698-701, Halifax, Canada.

de Moustier, C. and Alexandrou, D., 1991, "Angular dependence of 12 kHz seafloor acoustic backscatter", *JASA*, v.90, p.522-531.

Dugelay, S., Graffigne, C. and Augustin, J.M., 1996, "Deep seafloor characterization with multibeam echosounders by image segmentation using angular acoustic variations", *Proceedings SPIE*, vol 2823, pg. 255-266, Denver.

Haralick, R.M, 1979, "Statistical and Structural Approaches to Texture", *Proceedings of the IEEE*, vol. 67, n.5, p. 786-804.

Hellequin, L., Lurton, X. and Augustin, J.M., 1997, "Postprocessing and Signal Corrections for Multibeam Echosounder Images", *IEEE Oceans'97 Conference Proceedings*, vol. 1, p. 23-26, Halifax, Canada.

Hellequin, L., Boucher, J.M. and Lurton, X., 2003, "Processing of High-Frequency Multibeam Echo Sounder Data for Seafloor Characterization", *IEEE Journal of Oceanic Engineering*, vol. 28, no. 1, p. 78-89.

Hughes Clarke, J.E., 1994, "Toward remote seafloor classification using the angular response of acoustic backscattering: a case study from multiple overlapping GLORIA data", *IEEE Journal of Oceanic Engineering*, v.19, no.1, p.364-374.

Hughes Clarke, J.E., Danforth, B.W. and Valentine, P., 1997, "Areal Seabed Classification using Backscatter Angular Response at 95KHz", *High Frequency Canadian Hydrographic Conference 04 Conference Proceedings*, Lerici, Italy.

Hughes Clarke, J.E., 2004, "Seafloor Characterization Using Keel-mounted Sidescan: Proper Compensation for Radiometric and Geometric Distortion", *Canadian Hydrographic Conference 04 Conference* Proceedings, Ottawa, Canada.

Imen, K., Fablet, R., Boucher, J.M. and Augustin, J.M., 2005, "Statistical Discrimination of Seabed Textures in Sonar Images Using Co-Occurrence Statistics", *IEEE Oceans'2005 Conference Proceedings*, vol. 1, p. 605-610, Brest, France.

Kavli, T., Carlin, M. and Madsen, R., 1993, "Seabed Classification Using Artificial Neural Networks and Other Non-Parametric Methods", *Proceedings of the Institute of Acoustics, Acoustic Classification and Mapping of the Seabed*, v. 15, pt. 2, pp. 141–148, Bath, U.K.

Lurton, X., Dugelay, S. and Augustin, J.M., 1994, "Analysis of Multibeam Echo-Sounder Signals from the Deep Seafloor", *IEEE Oceans'94 Conference Proceedings*, vol. 3, p. 213-218, Brest, France.

Matsumoto, H., Dziak, R.P. and Fox, C., 1993, "Estimation of seafloor microtopographic roughness through modeling of acoustic backscatter data recorded by multibeam systems", *JASA,* v.94, p.2776-2787.

Pace, N.G. and Dyer, C.M., 1979, "Machine Classification of Sedimentary Sea Bottoms", *IEEE Transactions on Geoscience Electronics,* vol. GE-17, no. 3, p. 52–56.

Pace, N.G. and Gao, H., 1988, "Swathe Seabed Classification", *IEEE Journal of Oceanic Engineering,* vol. 13, no. 2, p. 83–90.

Quester Tangent, 2006, QTC Multiview product literature.

Reed, T.B. and Hussong, D. , 1989, "Digital image processing techniques for enhancement and classification of SeaMARC II side scan sonar imagery", *JGR*, v.84, B6, p.7469-7490.

Simrad, 1992, "Simrad EM1000. Hydrographic Echosounder: Product Description", Horten, Norway.

Tamsett, D., 1993, "Sea-Bed Characterization and Classification from the Power Spectra of Side-Scan Sonar Data", *Marine Geophysical Research*, v.15, p.43-64.